Cationic Cell-Penetrating Peptide Binds to Planar Lipid Bilayers Containing Negatively Charged Lipids but does not Induce Conductive Pores

Philip A. Gurnev,[†‡*] Sung-Tae Yang,[‡] Kamran C. Melikov,[‡] Leonid V. Chernomordik,[‡] and Sergey M. Bezrukov[‡]
[†]Department of Physics, University of Massachusetts, Amherst, Massachusetts; and [‡]Program in Physical Biology, Eunice Kennedy Shriver National Institute of Child Health and Human Development, National Institutes of Health, Bethesda, Maryland

ABSTRACT Using a cation-selective gramicidin A channel as a sensor of the membrane surface charge, we studied interactions of oligoarginine peptide R9C, a prototype cationic cell-penetrating peptide (CPP), with planar lipid membranes. We have found that R9C sorption to the membrane depends strongly on its lipid composition from virtually nonexistent for membranes made of uncharged lipids to very pronounced for membranes containing negatively charged lipids, with charge overcompensation at R9C concentrations exceeding 1 μM. The sorption was reversible as it was removed by addition of polyanionic dextran sulfate to the membrane bathing solution. No membrane poration activity of R9C (as would be manifested by increased bilayer conductance) was detected in the charged or neutral membranes, including those with asymmetric negative/neutral and negative/positive lipid leaflets. We conclude that interaction of R9C with planar lipid bilayers does not involve pore formation in all studied lipid combinations up to 20 μM peptide concentration. However, R9C induces leakage of negatively charged but not neutral liposomes in a process that involves lipid mixing between liposomes. Our findings suggest that direct traversing of CPPs through the uncharged outer leaflet of the plasma membrane bilayer is unlikely and that permeabilization necessarily involves both anionic lipids and CPP-dependent fusion between opposing membranes.

INTRODUCTION

Efficient intracellular delivery of biologically active macromolecules is crucial for a wide range of important medical problems, including delivery of macromolecular drugs to diseased cells and reprogramming somatic cells by transcription factors, to name just a few examples. Search for novel approaches of targeted drug delivery is greatly facilitated by the progress in understanding of the involved molecular interactions. Ironically, cationic cell-penetrating peptides (CPPs) such as oligoarginines are among the most extensively studied and practically used delivery vehicles for in vivo applications, but the mechanisms by which these very polar molecules cross biological membranes remain poorly understood.

Recently, several groups have suggested that interaction of CPPs with membranes results in formation of conductive pores through which CPPs and the associated cargo cross the membrane bilayer (1–3). Using molecular simulations and ionic current measurements on planar lipid bilayers, it was concluded (1,2,4) that cationic CPP nano-arginine (R9) interacts with the negatively charged and zwitterionic membranes inducing small conductive pores in both types of membranes. In contrast, a recent study (3) with another cationic CPP, TAT peptide has demonstrated that it induces leakage of encapsulated dye from liposomes containing negatively charged lipids such as dioleoyl phosphatidylglycerol (DOPG) and dioleoyl bis(monoacylglycero)phosphate (DOBMP), but not from liposomes containing only zwitterionic phospholipids lipids such as dioleoylphosphatidylcholine (DOPC) and cholesterol. Moreover, the results indicated that liposome leakage depends on TAT peptide-induced fusion between liposomes and is inhibited by treatments that prevent liposome fusion. Both models propose formation of transient conductive pores upon interaction of the peptide with membranes; however, different requirements for lipid composition and system topology in these models are very important for the delivery mechanism. Although the first model suggests that cationic CPPs may directly traverse plasma and endosomal membrane, the second model suggests that CPPs may only escape into cytosol after trafficking into multivesicular late endosomal compartments enriched in bis(monoacylglycero)phosphate.

Given the importance of this question for our understanding of interactions between cationic CPPs and membranes in cellular context, we extended the previous work to study interactions of R9C with negatively charged and uncharged membranes using two complementary experimental approaches. Our experiments on liposome suspension indicated that R9C-induced permeabilization of membranes detected as release of liposomal content was observed only for negatively charged membranes and correlated with fusogenic activity detected as lipid mixing. Measurements on planar lipid bilayers, using a cation-selective gramicidin A channel as a sensor of the surface membrane charge, have confirmed that R9C interacts only with negatively charged bilayers. However, even for these bilayers, R9C did not form conductive pores. These findings argue against the mechanism suggesting that interactions between R9C and the uncharged outer leaflet of plasma membrane

Submitted December 12, 2012, and accepted for publication February 27, 2013.

*Correspondence: gurnev@physics.umass.edu or gurnevp@mail.nih.gov

Editor: William Wimley.

0006-3495/13/05/1933/7 $2.00

http://dx.doi.org/10.1016/j.bpj.2013.02.053

bilayer permeabilize plasma membrane and substantiate the hypothesis that CPP enter cytosol by leaky fusion between negatively charged internal vesicles in multivesicular late endosomes.

MATERIALS AND METHODS

Large unilamellar vesicles (LUVs) of different lipid composition were prepared by extrusion. In brief, lipids dissolved in benzene/methanol (95:5, vol/vol) were freeze-dried under high vacuum overnight and the dried lipid powder was hydrated in an appropriate buffer at room temperature and then vortexed. The resulting lipid suspension was submitted to 10 successive cycles of freezing and thawing, and then extruded 10 times through two stacked Nucleopore polycarbonate filters of 100 nm pore size (Whatman, Piscataway, NJ) using a LIPEX extruder (Northern Lipids, Burnaby, Canada) to produce LUVs. Liposome sizes were measured using dynamic light scattering on an N4Plus submicron particle size analyzer (Beckman Coulter, Brea, CA). Lipid mixture mimicking the phospholipid composition of intraluminal vesicles of late endosomes (ILM) contained DOBMP, 1,2-dioleoyl-*sn*-glycero-3-phosphocholine (DOPC), and 1,2-dioleoyl-*sn*-glycero-3-phosphoethanolamine (DOPE) in 77:19:4 molar ratio. Lipid mixture mimicking the lipid composition of the outer leaflet of the plasma membrane (CPM) contained DOPC, DOPE, sphingomyelin, and cholesterol in 1:1:1:1.5 molar ratio. All lipids were purchased from Avanti Polar Lipids (Alabaster, AL).

To measure content release, liposomes were prepared in a buffer containing 1 mM small water-soluble fluorescent dye 8-hydroxypyrene-1,3,6-trisulfonic acid (HPTS, Invitrogen, Eugene, OR), 5 mM quencher *p*-xylene-bis-pyridinium bromide (DPX, Invitrogen), 130 mM NaCl, 10 mM HEPES, pH 7.4. After extrusion, not encapsulated dye and a quencher were removed by size exclusion chromatography using a PD-10 desalting column (Amersham Biosciences, Piscataway, NJ). Fluorescence changes induced by different concentrations of R9C peptide (SynPep, Dublin, CA) were recorded in disposable methacrylate 10 mm pathlength cuvettes in 2 mL of buffer under constant stirring using a Bowman-2 luminescence spectrometer (Aminco, Rochester, NY) with $\lambda ex = 416.4$ nm and $\lambda em = 520$ nm. The extent of content leakage was calculated according to the following equation: $\%\ \text{Leakage} = 100 \times (F(t) - F0)/(F\text{triton} - F0)$, where F(t), F0, and Ftriton are fluorescence intensities at time t, before addition of peptide and after the complete release of encapsulated dye by addition of 0.1% v/v of Triton X-100.

R9C peptide-induced lipid mixing was measured by the dequenching of *N*-(lissamine Rhodamine B sulfonyl)-phosphatidylethanolamine (Rh-PE, Avanti Polar Lipids) fluorescence. Unlabeled liposomes of different lipid composition and liposomes labeled with a self-quenching concentration (5 mol %) of Rh-PE were prepared in 150 mM NaCl, 10 mM HEPES, pH 7.4 buffer. Liposomes were added to a cuvette in a ratio of 1:10 of labeled to unlabeled liposomes for a total lipid concentration of 25 μM. Different concentrations of R9C peptide were added to induce lipid mixing between liposomes. All experiments were performed at room temperature. Lipid mixing between liposomes results in a dilution of Rh-PE and an increase in dye fluorescence due to a relief of self-quenching. Fluorescence changes induced by R9C were recorded in disposable methacrylate 10 mm pathlength cuvettes in 2 mL of buffer under constant stirring using a Bowman-2 luminescence spectrometer (Aminco) with $\lambda ex = 560$ nm and $\lambda em = 585$ nm. At the end of each recording, complete dequenching of the dye was induced by addition of Triton X-100 (0.1% v/v final concentration). The degree of dye quenching was calculated as $Q(t) = 100 \times (F(t) - F0)/(F\text{triton} - F0)$, where F(t), F0, and Ftriton are fluorescence at time t, before addition of peptide and after addition of Triton X-100, respectively. Lipid mixing was inhibited by replacing 2 mol% of PC in the basal ILM lipid mixture with 2 mol% of 1,2-dioleoyl-*sn*-glycero-3-phosphoethanolamine-N-[methoxy(polyethylene glycol)-2000] (PEG-DOPE, Avanti Polar Lipids).

Bilayer lipid membranes were prepared from DOBMP, DOPC, a 1:1 mixture of these lipids, 1,2-diphytanoyl-*sn*-glycero-3-phosphocholine (DPhPC), and from 1,2-dioleoyl-3-trimethylammonium-propane (DOTAP), Avanti Polar Lipids, using a modified (5) monolayer-opposition technique by Montal and Mueller (6). Uncharged DOPC and DPhPC membranes were used interchangeably. The Teflon chamber, with two (*cis* and *trans*) compartments of 2 ml, was divided by a 15-μm-thick Teflon partition with a 60–70-μm diameter aperture, with the actual diameter of the bilayer reduced by the contact torus. Lipid monolayers were made from 2 mg/ml aliquots of lipids in pentane. After bilayer formation R9C peptide was added in the 1 nM–10 μM range to the *cis* only or both compartments from the 1 mM stock in 150 mM CsCl, 5 mM HEPES, pH 7.4. Gramicidin A (a generous gift from O. S. Andersen, Weill Cornell University Medical College) was added from 1 to 10 nM ethanol stock solutions to both aqueous compartments at the amount sufficient to produce single channels. To neutralize R9C, dextran-sulfate (average molecular mass of 8000, Sigma, St. Louis, MO) was added directly to the R9C-containing chamber compartment(s) from the 10 mM stock solution 150 mM CsCl, 5 mM HEPES at pH 7 to the final concentration of 50 μM.

The applied voltage was maintained using Ag/AgCl electrodes with 2 M KCl and 15% (w/v) agarose bridges. The voltage was designated as positive if potential was higher on the *cis* side of the membrane, the side of oligoarginine addition. The membrane chamber and headstage were isolated from external noise sources with a double metal screen (Amuneal Manufacturing, Philadelphia, PA). Conductance measurements were performed using an Axopatch 200B amplifier (Molecular Devices, Foster City, CA) in the voltage clamp mode. Data were filtered by a low-pass 8-pole Butterworth filter (model 9002, Frequency Devices, Haverhill, MA) at 15 kHz, directly saved into the computer memory with a sampling frequency of 50 kHz, and analyzed using pClamp 10 software. All measurements were made at room temperature, $T = (23 \pm 1)^\circ C$. Amplitudes of current steps corresponding to formation and dissociation of single gramicidin A channels were collected at a given transmembrane voltage and their histograms of ~50 single events were fitted by a Gaussian distribution.

RESULTS

First, we tested the ability of R9C to induce release of encapsulated water soluble dyes from liposomes of different lipid compositions and whether this release is accompanied by lipid mixing. Fig. 1 shows that R9C efficiently induced leakage from negatively charged ILM liposomes with lipid composition mimicking that of intraluminal late endosomal vesicle membrane but not from uncharged CPM liposomes with lipid composition mimicking lipid composition of cell plasma membrane. When we measured R9C-induced fusion between liposomes using lipid mixing assay as illustrated by Fig. 2, we observed fusion only in the case of ILM liposomes but not in the case of CPM liposomes. Furthermore, when lipid mixing was inhibited by incorporation of a small amount of PEG-grafted lipid into the lipid composition of ILM liposomes (Fig. 2 *B*), we observed a significant inhibition of liposome leakage (Fig. 1 *C*). Altogether, these results are consistent with our previous observations for TAT peptide (3) and indicate that CPP-induced liposome leakage is dependent on the presence of anionic lipids and, importantly, on CPP-induced fusion between liposomes.

Our dye leakage assay is limited by the size of encapsulated fluorescent dye (molecular mass of HPTS is 300 Da), because we are able to detect only pores that are large

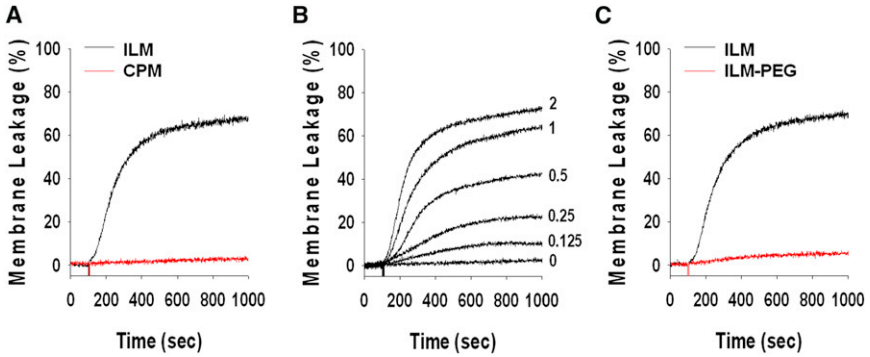

FIGURE 1 Release of encapsulated probe from liposomes induced by oligoarginine R9C requires the presence of negatively charged lipids but can be blocked by PEGs attached to lipid polar heads. (*A*) Kinetics of dye dequenching due to release of HPTS/DPX from 50 μM liposomes of ILM (*black trace*) or CPM (*red trace*) lipid composition upon addition of 2 μM R9C. R9C releases encapsulated probe from ILM-liposomes but not from CPM-liposomes. (*B*). Dependence of dye dequenching due to the release of HPTS/DPX from 50 μM liposomes of ILM-lipid composition on peptide concentration. Traces are labeled with the concentration (in μM) of the added R9C. (*C*) Effects of PEG-PE incorporation on kinetics of R9C (2 μM) induced dye dequenching due to release of HPTS/DPX from liposomes (50 μM). Liposome lipid composition was modified by replacing 2 mol% of PC in basal ILM lipid mixture with 2 mol% of PEG-PE.

enough to allow HPTS passage. Therefore, we used a significantly more sensitive approach of electrical measurements on planar lipid bilayers to test if R9C can induce conductive pores in a free-standing membrane. But first we characterized binding of the R9C peptide to membranes of different composition using a cation-selective channel produced by the benchmark antibiotic gramicidin A as a single-molecule sensor of the membrane surface charge. Recently, this approach was used to evaluate the sorption of trivalent cations to the negatively charged membranes (7). It was shown that the sorption of counterions compensates and, at certain concentrations, even overcompensates the initial negative charge of membrane surface, which leads to the change in the sign of membrane surface potential.

In lipid bilayers gramicidin A forms narrow channels that are ideally selective for monovalent cations (8). For this reason its conductance is very sensitive to the membrane surface potential, which modulates the concentration of cations at the channel entrance. In its own turn, the membrane surface potential depends on the surface charge and a degree of its modification by the adsorbed charged species. Fig. 3 shows that the addition of R9C to the membrane-bathing solution of a negatively charged membrane reduces the Cs^+ current through the gramicidin A channel in a concentration-dependent manner. The current records in Fig. 3 *A* give raw data showing that R9C reduces the magnitude of the current steps that correspond to formation and dissociation of individual channels. The effect is due to R9C-induced reduction of the absolute value of the negative membrane potential and, therefore, reduction in the concentration of Cs^+ at the channel entrance.

Similar to the findings for trivalent cations (7), oligoarginine R9C, carrying nine positive charges, not only compensates the charge of the negatively charged membranes, but, at R9C concentrations exceeding 1 μM, overcompensates it by changing the sign of the membrane surface charge. This is demonstrated by the data in Fig. 3 *B*, which show that, starting from these concentrations, the current through the channel gets smaller than the current in a neutral (DOPC) lipid designated by the second horizontal dotted line. As the concentration of R9C increases, the current approaches its value for a positively charged lipid (DOTAP) shown by the third dotted line from the top. The data in Fig. 3 *B* combined with the analytical considerations given elsewhere (7), allow us to calculate the R9C adsorption isotherm yielding the dissociation constant of ~0.5 μM.

Fig. 4 shows that R9C sorption strongly depends on membrane lipid composition and changes from negligible for pure DOPC membranes to a highly pronounced one in pure DOBMP membranes. Indeed, within the experimental error addition of 1 μM R9C to the membrane-bathing solution did not change the current through the channel in membranes formed from pure DOPC (*leftmost points on the graph*). In the absence of R9C progressive admixing of DOBMP increases channel conductance (*open circles*, control) because the negative charge of DOBMP attracts Cs^+ counterions and increases their concentration at the channel entrance. However, in the presence of 1 μM R9C the effect

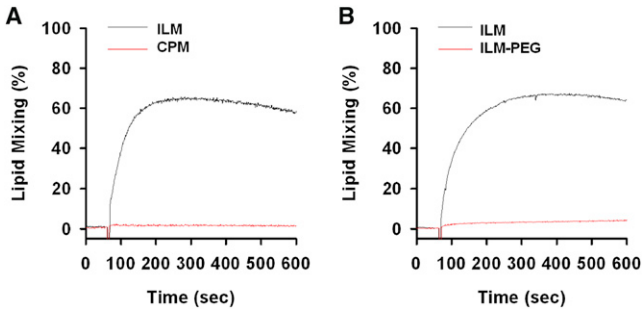

FIGURE 2 R9C induces lipid mixing between liposomes. (*A*) The kinetics of Rh-PE dequenching due to lipid mixing between ILM- (*black trace*) and CPM- (*red trace*) liposomes (50 μM final total lipid concentration) induced by 2 μM R9C. (*B*) Effects of PEG-PE incorporation on kinetics of R9C (2 μM) induced Rh-PE dequenching due to lipid mixing between liposomes (50 μM). Liposome lipid composition was modified as described in the Fig. 1 caption.

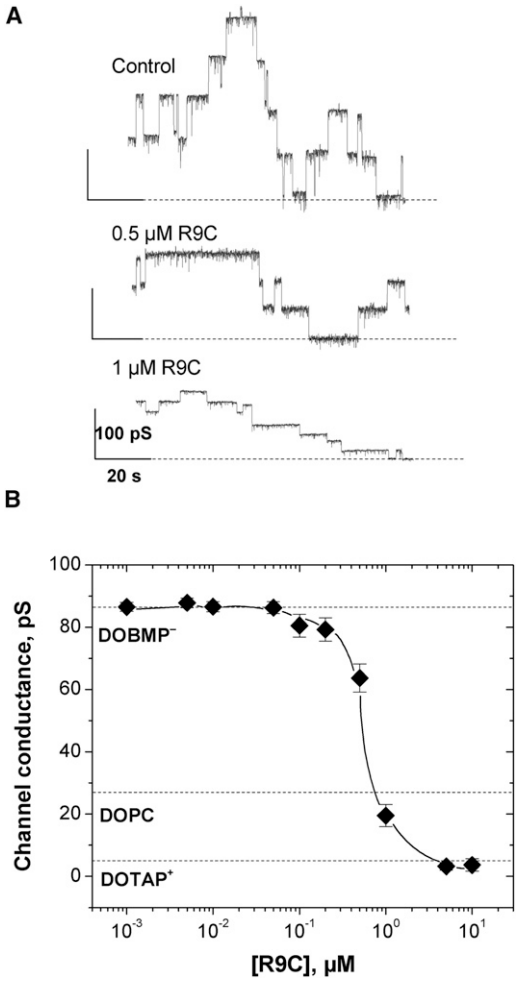

FIGURE 3 Effect of symmetric addition of oligoarginine CPP R9C on single-channel conductance of gramicidin A in planar lipid membrane from negatively charged lipid DOBMP reveals strong sorption of R9C to the membrane surface. Membrane buffer contained 150 mM CsCl, 5 mM HEPES, pH 7.4, the applied voltage was 100 mV. Panel *A* shows traces of single gramicidin A channel fluctuations as the solution concentration of R9C was increased. Panel *B* summarizes the data of the titration experiments. Single-channel conductance remains unchanged as the bulk concentration of R9C stays below 100 nM, but then quickly decreases. Horizontal dashed lines denote the channel conductance for the negatively charged DOBMP, zwitterionic DOPC, and positively charged DOTAP. Judging by single-channel conductance at R9C concentration ≥ 1 μM, the negative membrane surface is not only neutralized by cationic CPP (at ~0.6 μM), but becomes positively charged with the charge density of DOTAP membranes.

of DOBMP admixing on conductance is the opposite. The lipid-dependent sorption of R9C overcompensates the negative charge of DOBMP, which is seen as a reduction of the channel current relative to its value in pure DOPC membranes, in accord with the data in Fig. 3.

The sorption of R9C was reversible because it could be completely removed by the addition of an R9C-binding agent. Fig. 5 shows that the highly asymmetric current-voltage curve characteristic of the channel in asymmetrically charged membranes (7) not only could be made nearly

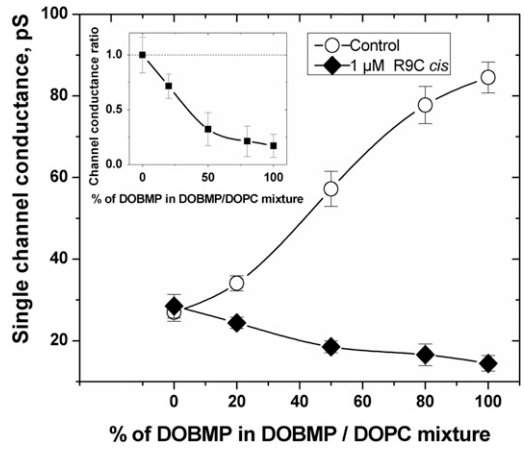

FIGURE 4 Adsorption of R9C depends strongly on the content of the negatively charged lipid (DOBMP). The graph shows the effect of 1 μM *cis* side R9C addition on the single-channel gramicidin A conductance, recorded at V = +100 mV in the specified membranes. In the absence of R9C the channel conductance increases proportionally to the DOBMP content in DOBMP/DOPC lipid mixture (*open circles*); however, addition of R9C reduces the channel conductance even beyond its value in the neutral lipid (*solid diamonds*). The inset gives the ratio of the channel conductances in the absence and presence of R9C. Membrane buffer contained 150 mM CsCl, 5 mM HEPES, pH 7.4.

symmetric by the R9C addition, but were completely restored by the consequent application of polyanionic dextran sulfate to the membrane-bathing solution.

Thus, the adsorption of a model cell-penetrating peptide R9C to the bilayer membrane was carefully controlled in our experiments. However, we were unable to detect any

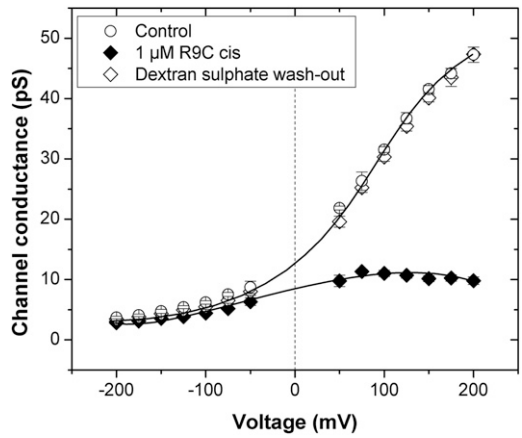

FIGURE 5 The adsorption of R9C does not affect lipid mixing in the asymmetric DOBMP/DOPE (4:1) *cis*//DOTAP *trans* bilayer, as probed with gramicidin A channel conductance (R9C was applied from the *cis* side). In the asymmetric membrane the current through a single channel is highly asymmetric in voltage (*open circles*, see also (7)). Application of 1 μM R9C produces a strong effect on the channel current at the applied voltages positive from the DOBMP/DOPE leaflet side (*solid squares*). However, the adsorbed R9C can be effectively removed from the membrane surface by applying polyanionic dextran sulfate (50 μM) so that the initial asymmetric current-voltage curve is restored (*open diamonds*). Membrane buffer contained 150 mM CsCl, 5 mM HEPES, pH 7.4.

pore formation by R9C in any of the lipid compositions used in this study. In the absence of gramicidin, R9C addition to the membrane bathing solution did not induce any increases in the membrane conductance. Fig. 6 and Table 1 summarize our effort. Fig. 6 *A* shows that the current through the DOBMP membranes in the absence (*upper track*) and presence (*lower track*) of 20 μM R9C are nearly identical and correspond to ~0.03 pA leakage current at 100 mV applied voltage. Of importance, the oligoarginine concentration in this experiment is an order of magnitude higher than its highest concentration used in the dye-releasing and lipid-mixing experiments of Figs. 1 and 2.

The time resolution in the experiments, examples of which are shown in Fig. 6 *A* and summarized in Table 1, was limited to 0.1 s. This was done to increase the current resolution to ~0.01 pA. It is seen that there are no events of this or higher amplitude at the timescales larger than the resolution time. To address a possibility of R9C generating much shorter and rare events that could be missed with such analysis, we performed power spectral measurements of current noise using the filter frequency of 15 kHz, which corresponds to ~10 μs time resolution. Fig. 6 *B* shows that the noise spectra for the membranes in the presence and absence of 20 μM R9C coincide. In the frequency range from 10 to 1000 Hz they do not differ by more than a fraction of 10^{-5} pA^2/Hz. This allows us to give an upper estimate for the amplitude of the events that could have been missed at 0.1 s resolution. Indeed, considering the case of short events with low repetition rate ν and amplitude i, one can estimate the power spectral density as (5)

$$S_i(f) = \frac{4i^2\tau^2\nu}{1+(2\pi f\tau)^2}, \quad (1)$$

where f is frequency and τ is the average lifetime of the events. For small lifetimes, $\tau \ll f$, this gives the following limitation on the amplitude, lifetime, and repetition rate

$$i^2\tau^2\nu \leq 10^{-6}\text{pA}^2\text{s}. \quad (2)$$

As an example, for hypothetical events with the repetition rate of one per second and the lifetime of 1 ms, the estimate gives $i \leq 1$ pA.

Thus, we find that despite the well-pronounced binding to the negatively charged membranes, clearly monitored with gramicidin A conductance, R9C does not induce any transient pores or measurable increase in the membrane ionic leakage in the negatively charged or neutral membranes including membranes of asymmetric structure with negative/positive lipid leaflets (Fig. 6 and Table 1). These results are consistent with the model suggesting that membrane poration by cationic CPP happens only concomitantly with CPP-induced membrane fusion (3).

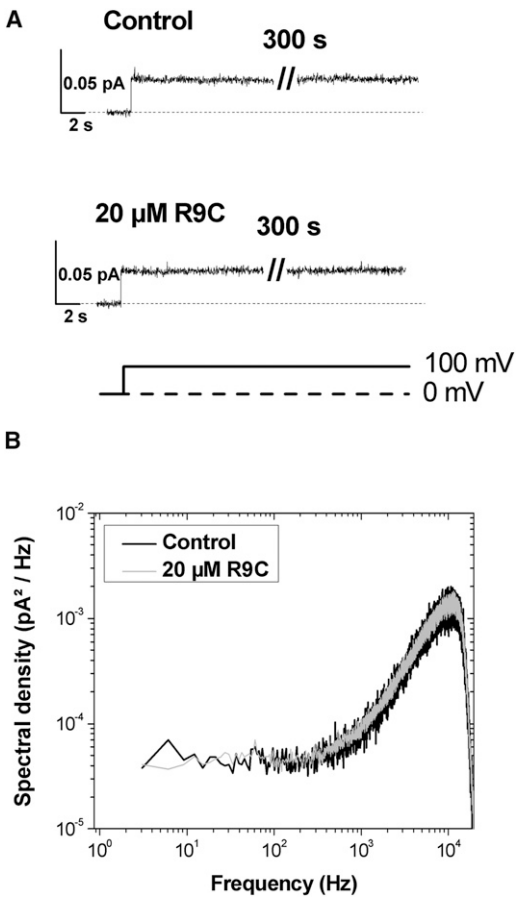

FIGURE 6 The adsorption of R9C does not induce any measurable destabilization and/or ionic permeabilization of the membrane made from negatively charged DOBMP. The panel *A* gives two consecutive current traces as 100 mV was applied to DOBMP membrane before and after R9C addition in concentration of 20 μM applied from the *cis* side. The amplifier was in the Patch configuration. Panel *B* presents a nearly perfect overlap of the noise spectra for the membranes in the presence and absence of R9C. The amplifier was in the Whole Cell configuration. Membrane buffer contained 150 mM CsCl, 5 mM HEPES, pH 7.4.

DISCUSSION

Despite significant efforts, the mechanisms by which cationic CPPs cross lipid bilayers and enter cell cytosol remain poorly understood. A large body of data accumulated from experiments both on living cells and artificial lipid membranes did not lead to emergence of a single generally accepted model of CPP translocation across the membrane but rather resulted in formulation of a number of different hypotheses (1,3,9–13). Our results, together with the previously published data (3,14), indicate that different cationic CPPs can induce formation of ion-conducting structures in membranes, but that such activity requires both the presence of anionic lipids in the membrane and CPP-dependent fusion of opposing membranes. Although the mechanism of CPP-dependent leaky fusion remains to be explored, recent study suggested that fusogenic activity of cationic CPPs may be attributed to their ability to induce clustering of anionic

TABLE 1 The absence of the measurable effect of addition of 10 μM oligoarginine on ionic conductance of planar lipid bilayers of different lipid compositions

			Trans monolayer		
			$DOBMP^-$	DPhPC	$DOTAP^+$
Cis monolayer	$DOBMP^-$	*Control*	0.06 ± 0.036 pA	0.09 ± 0.05 pA	0.08 ± 0.04 pA
		R9C 10 μM	0.06 ± 0.04 pA	0.10 ± 0.06 pA	0.075 ± 0.04 pA
	DPhPC	*Control*	0.12 ± 0.07pA	0.15 ± 0.055 pA	0.13 ± 0.06 pA
		R9C 10 μM	0.09 ± 0.06 pA	0.12 ± 0.06 pA	0.13 ± 0.05 pA
	$DOTAP^+$	*Control*	0.08 ± 0.04 pA	0.13 ± 0.06 pA	0.23 ± 0.06 pA
		R9C 10 μM	0.07 ± 0.04 pA	0.13 ± 0.06 pA	0.25 ± 0.06 pA

Transmembrane currents through bilayers formed over a ~70 μm diameter aperture in 0.15 M CsCl were measured in the absence and presence of oligoarginine from the *cis* side at 100 mV applied voltage. Standard error was calculated from 3 to 4 experiment replications.

lipids (15). In cellular context, cationic CPPs and CPP-cargo conjugates have to be first endocytosed and trafficked to reach the lumen of multivesicular late endosomes before they can escape by inducing leaky fusion between BMP-containing membranes of internal vesicles of late endosome and between internal vesicles and limiting membrane of late endosomes. The peptide/lipid ratios, at which we observed the leakage (1:400 to 1:25), can be comparable to the peptide/lipid ratios in the endosomes. Cellular uptake of cationic peptides is preceded by their accumulation at heparan sulfate proteoglycans on the cell surface (16). We used reported cell surface density of heparan sulfate receptor (17) to estimate that peptide/lipid ratios within endosomes can be as high as 1:100 to 1:20. Clearly, contributions of the leaky fusion mechanism into endosomal escape of CPPs remain to be evaluated by experiments on cells.

Cationic CPPs added to free-standing negatively charged lipid bilayers did not induce pore formation despite strong binding to such membranes as manifested by recharging of the initially negatively charged membrane surface to the positive one. In the absence of negatively charged lipids we observed neither binding of R9C peptide nor pore formation. These results are in contradiction with the data previously published by Herce and co-authors (2). Of importance, we are confident that the sensitivity of our measurements would allow us to detect the presence of very small and short-living pores as evidenced by our ability to characterize the small channel formed by gramicidin A with the high time and conductance resolution demonstrated previously.

Our results suggest that it is unlikely that interactions of cationic CPPs with plasma membrane of the cell may lead to formation of pores. It is more feasible that CPPs may induce pore formation once they reach late endosomal compartments where the presence of negatively charged BMP and the multivesicular structure of the organelle facilitates CPP interaction with the membrane ultimately leading to peptide and cargo release into the cytosol. Indeed, this remains to be experimentally demonstrated in the living cells. We also observed that binding of cationic CPP to the membrane surface is able to strongly modulate the conductance of ion channels. Based on this result, one may propose that upon binding to the cell surface proteoglycans cationic CPPs may affect properties of cellular channels in plasma membrane to induce complex biological responses to CPP such as rearrangements of cortical actin cytoskeleton (18).

To conclude, we demonstrate that oligoarginine R9C does not induce ion-conductive structures in planar lipid bilayers even in the case of the negatively charged bilayers that avidly bind the peptide. Although 0.2–2 μM concentrations of oligoarginine were found to be enough for induction of the efficient encapsulated probe release of (Fig. 1) or lipid mixing (Fig. 2) in liposome experiments, we show that order of magnitude higher R9C concentrations do not porate membranes (Fig. 6 and Table 1). Though the reasons of the discrepancy between the present results and those reported by Herce and co-authors (2) are not clear at the moment, it is appropriate to mention that instances of spontaneous conductive structure formation have been described for pure lipid bilayers in the absence of any known channel-formers and attributed to either lipid oxidization (19) or small amounts of unidentified admixtures (20), or lipid phase transitions (21) and a recent review (22), or the effects of strong electric fields (23). One may suggest that under certain appropriate conditions CPPs could promote formation of these poorly understood conductive defects. Nevertheless, our work demonstrates that neither the presence of CPP in solution, nor its sorption to the membrane surface constitute a sufficient condition for ion-conductive structure formation in neutral, negatively charged, positively charged, or asymmetrical membranes. This allows us to assert that permeabilization requires the presence of negatively charged lipids but occurs in a process that involves fusion between opposing membranes, suggesting that in a cellular context trafficking to multivesicular late endosomes is a necessary step in peptide delivery to cytosol.

This study was supported by the Intramural Research Program of the National Institutes of Health (NIH), Eunice Kennedy Shriver National Institute of Child Health and Human Development.

REFERENCES

1. Herce, H. D., and A. E. Garcia. 2007. Molecular dynamics simulations suggest a mechanism for translocation of the HIV-1 TAT peptide across lipid membranes. *Proc. Natl. Acad. Sci. USA.* 104:20805–20810.

2. Herce, H. D., A. E. Garcia, …, V. Milesi. 2009. Arginine-rich peptides destabilize the plasma membrane, consistent with a pore formation translocation mechanism of cell-penetrating peptides. *Biophys. J.* 97:1917–1925.

3. Yang, S. T., E. Zaitseva, …, K. Melikov. 2010. Cell-penetrating peptide induces leaky fusion of liposomes containing late endosome-specific anionic lipid. *Biophys. J.* 99:2525–2533.

4. Huang, K., and A. E. García. 2013. Free energy of translocating an arginine-rich cell-penetrating peptide across a lipid bilayer suggests pore formation. *Biophys. J.* 104:412–420.

5. Bezrukov, S. M., and I. Vodyanoy. 1993. Probing alamethicin channels with water-soluble polymers. Effect on conductance of channel states. *Biophys. J.* 64:16–25.

6. Montal, M., and P. Mueller. 1972. Formation of bimolecular membranes from lipid monolayers and a study of their electrical properties. *Proc. Natl. Acad. Sci. USA.* 69:3561–3566.

7. Gurnev, P. A., and S. M. Bezrukov. 2012. Inversion of membrane surface charge by trivalent cations probed with a cation-selective channel. *Langmuir.* 28:15824–15830.

8. Koeppe, 2nd, R. E., and O. S. Anderson. 1996. Engineering the gramicidin channel. *Annu. Rev. Biophys. Biomol. Struct.* 25:231–258.

9. Magzoub, M., A. Pramanik, and A. Gräslund. 2005. Modeling the endosomal escape of cell-penetrating peptides: transmembrane pH gradient driven translocation across phospholipid bilayers. *Biochemistry.* 44:14890–14897.

10. Binder, H., and G. Lindblom. 2003. Charge-dependent translocation of the Trojan peptide penetratin across lipid membranes. *Biophys. J.* 85:982–995.

11. Sakai, N., T. Takeuchi, …, S. Matile. 2005. Direct observation of anion-mediated translocation of fluorescent oligoarginine carriers into and across bulk liquid and anionic bilayer membranes. *ChemBioChem.* 6:114–122.

12. Terrone, D., S. L. W. Sang, …, J. R. Silvius. 2003. Penetratin and related cell-penetrating cationic peptides can translocate across lipid bilayers in the presence of a transbilayer potential. *Biochemistry.* 42:13787–13799.

13. Marks, J. R., J. Placone, …, W. C. Wimley. 2011. Spontaneous membrane-translocating peptides by orthogonal high-throughput screening. *J. Am. Chem. Soc.* 133:8995–9004.

14. Melikov, K., and L. V. Chernomordik. 2005. Arginine-rich cell penetrating peptides: from endosomal uptake to nuclear delivery. *Cell. Mol. Life Sci.* 62:2739–2749.

15. Wadhwani, P., R. F. Epand, …, R. M. Epand. 2012. Membrane-active peptides and the clustering of anionic lipids. *Biophys. J.* 103:265–274.

16. Richard, J. P., K. Melikov, …, L. V. Chernomordik. 2005. Cellular uptake of unconjugated TAT peptide involves clathrin-dependent endocytosis and heparan sulfate receptors. *J. Biol. Chem.* 280:15300–15306.

17. Höök, M., L. Kjellén, and S. Johansson. 1984. Cell-surface glycosaminoglycans. *Annu. Rev. Biochem.* 53:847–869.

18. Nakase, I., M. Niwa, …, S. Futaki. 2004. Cellular uptake of arginine-rich peptides: roles for macropinocytosis and actin rearrangement. *Mol. Ther.* 10:1011–1022.

19. Yafuso, M., S. J. Kennedy, and A. R. Freeman. 1974. Spontaneous conductance changes, multilevel conductance states and negative differential resistance in oxidized cholesterol black lipid membranes. *J. Membr. Biol.* 17:201–212.

20. Gögelein, H., and H. Koepsell. 1984. Channels in planar bilayers made from commercially available lipids. *Pflugers Arch.* 401:433–434.

21. Antonov, V. F., V. V. Petrov, …, A. S. Ivanov. 1980. The appearance of single-ion channels in unmodified lipid bilayer membranes at the phase transition temperature. *Nature.* 283:585–586.

22. Heimburg, T. 2010. Lipid ion channels. *Biophys. Chem.* 150:2–22.

23. Melikov, K. C., V. A. Frolov, …, L. V. Chernomordik. 2001. Voltage-induced nonconductive pre-pores and metastable single pores in unmodified planar lipid bilayer. *Biophys. J.* 80:1829–1836.